Curriculum Vitae

APARNA BAXI

Email: aparna.baxi@umaryland.edu

EDUCATION

Master of Science (MS) in Molecular Medicine 2013

University of Maryland, Baltimore (UMB), Maryland

Thesis: Lymph node structure change following tolerance induction and immunization

Bachelor of Engineering (B.E) in Biotechnology 2010

Birla Institute of Technology, Mesra (BIT Mesra), Ranchi, India

Project: Study of two component response regulatory genes in rice (Oryza sativa) under anoxia.

TECHNICAL SKILLS

Molecular Biology techniques: Isolation of DNA, Agarose gel electrophoresis, Quantative RT-PCR, Molecular cloning, 2-D PAGE.

Immunology techniques: Immunohistochemistry, FACS, Sandwich ELISA, Affinity chromatography, Flow cytometry

Imaging techniques: Fluorescent microscopy

Animal work: Mouse injections- Tail vein, Intra peritoneal, subcutaneous; dissection with focus on peripheral lymphoid organs.

Culture techniques: Plant tissue culture, Bacterial cultures, Fungal cultures: Solid, Liquid and Submerged state fermentation, enzyme production and isolation.

Bioinformatics: Velocity Image analysis software, Clustal W/X, VMD - Visual Molecular Dynamics software, Prism-GraphPad, BLAST, PHYLIP (PHYlogeny Inference Package)

ACADEMIC PROJECTS

Tolerance induction changes Lymph node structure and function.

University of Maryland, Baltimore, March'12 – current

Restoring immune function of tumor-specific CD4+ T cells during recurrence of melanoma

University of Maryland, Baltimore, Febuary-March'12

(lab rotation)

Study of two component response regulatory genes in rice (Oryza sativa) under anoxia.

Birla Institute of Technology, Ranchi, India (January'09-April'10)

TRAINING PROJECTS

Study and chacterization of malignant cells with respect to normal cells.

Amolak diagnostics, Udaipur, India (November'10)

Effect of Lactic Acid Bacteria (LAB) on bacterial food pathogens.

Central Food and Dairy Science Department, Udaipur, India June'09

CONFERENCE PRESENTATIONS

Aparna Baxi, Bryna Burrell, Jonathan Bromberg; "**Tolerance induction changes Lymph node structure and function**", American Transplantation Congress (ATC) 2013, Seattle, WA, USA (Poster presentation)

Aparna Baxi, Bryna Burrell, Jonathan Bromberg; "**Tolerance induction changes Lymph node structure and function**", Graduate Research Conference-2013, University of Maryland Baltimore (Oral resentation)

Ashutosh Kumar, **Aparna Baxi**, Sneha Agarwal, Dev Mani Pandey.**"Study on molecular Mechanisms towards Submergence tolerance in Rice (Oryza sativa) : A Functional Genomics Approach"** Proceedings of National Seminar on Applications of Biotechnology & Development of Bihar-2010, Birla Institute of Technology, Patna, Bihar, India.

Samyukta B., Sneha Agarwal, **Aparna Baxi**, Annu Singh, Pratyoosh Shukla. **"Approaches in enzyme engineering through in silico modeling for improvement in catalytic binding site onsome microbial enzymes: an overview"**50th Annual Conference- 2009 conducted by National Chemical Laboratory, Pune, India.

Ashutosh Kumar, **Aparna Baxi**, Sneha Agarwal, Dev Mani Pandey **. "Expression Analysis of Two Component System Genes in Rice *(Oryza sativa . L)*"** Proceedings of 6th Rice Genetics Symposium and 7th international Symposium on Rice Functional Genomics (ISRFG'2009), Manila, Philippines,

PUBLICATIONS AND MANUSCRIPTS

Stephen Goding, Kyle Wilson, Ying Xie, Kristina Harris, Aparna Baxi, Akgu Akpinarli, Amy Fulton, Koji Tamada, Scott E. Strome, and Paul Andrew Antony. **Restoring immune function of tumor-specific CD4+ T cells during recurrence of melanoma**.(Submitted)

ABSTRACT

Thesis Title: Lymph node structure change following tolerance induction and immunization

Name of Candidate: Aparna Baxi

Thesis Advisor: Dr. Jonathan S Bromberg, Professor, Microbiology and Immunology

Background

Costimulatory blockade plus donor-specific transfusion (DST) induces long-term graft acceptance, however the mechanism by which this tolerance occurs remains incompletely defined. The lymph node (LN) contains a basic scaffolding structure comprised of collagens, laminins and stromal fibers such as ER-TR7. These fibers form a protein meshwork foundation for cell interactions and bind chemokines that guide cells to specific, instructive microdomains. This study tested the hypothesis that tolerance induction or immunization involves modification of lymph node structure and chemokine expression, which affect the localization of graft reactive T cells.

Methods

Tolerance was induced by treating C57BL/6 mice with BALB/c DST + anti-

CD40L mAb, while immunity was induced by treating mice with DST only. Mice were euthanized 12 hours to 7 days post-treatment and LNs were studied by quantitative immunohistochemistry or quantitative RT-PCR to define the amount and location of the structural elements collagen III, ER-TR7, desmin, laminin, the chemokines CCL19 and CCL21 and localization of graft reactive cells.

Results

LN in tolerant and immune mice displayed distinct structural modifications and chemokine expression. In the LN of tolerant mice, ER-TR7 increased and peaked at day 5 post-tolerance induction while, it remained close to levels observed in naïve LNs following immunization. Following tolerance induction or immunization, an increase in laminin, desmin and collagen III occurred. With respect to chemokines, CCL19 presence increased gradually after day 3 in tolerant mice. In contrast, CCL19 presence peaked at day 3 in immune mice. Interestingly, CCL21 presence decreased following both tolerance induction and immunization. At 12 hours post treatment, LN follicular reticular cells (FRCs) from tolerant LNs seemed to express higher amounts of CCL21 as compared to immune FRCs that expressed CCL19. Graft reactive cells accumulated gradually in LN cortical ridge and T cell areas for tolerant LNs as compared to immune LNs.

Conclusion

Tolerance induction results in structural changes within the LN. ER-TR7 and laminin are essential LN structural stromal fibers, and CCL19 is important for T

cell and dendritic cell LN chemoattraction. These results suggest that tolerance induction leads to changes in both LN structure and function. These changes can subsequently affect T cell migration, homing and differentiation in the LN. Hence, this remodeling choreographs the encounters and interactions between antigen reactive cells and their cognate antigen resulting in tolerance as opposed to immunity. These findings suggest that the LN is a malleable structure, and changes in both physical structure and chemokine expression affect LN function.

Lymph node structure change following tolerance induction and immunization

By

Aparna Baxi

Thesis submitted to the faculty of the Graduate School of the
University of Maryland, Baltimore in partial fulfillment
of the requirements for the degree of
Master of Science
2013

ACKNOWLEDGEMENTS:

During the course of my masters program, I have been fortunate to work with many outstanding scientists. I owe my deepest gratitude to Dr. Jonathan S. Bromberg, for giving me an opportunity to work in his lab with his team of distinguished immunologists. I am grateful to Dr. Bryna Burrell for her constant guidance, support and patience while mentoring me throughout the course of this research project. I am highly thankful to my colleagues, Dr. Yumi Nakayama, Dr. Charles Brinkman, Dr. Daiki Iwami, Dr. Kristi Warren, Dr. Yanboa Xiong, Usha Rai and JuanJuan Zhao for their suggestions and help that were highly useful for my research.

I would also like to thank my thesis committee members Dr. Li Zhang, Dr. Gregory Carey and Dr. Frank Margolis for their august insights on the thesis and constant patience and support.

Last, but not the least, I would like to thank my family and friends for providing me the emotional and moral support, without which this Masters degree would not have been possible.

Table of contents

CHAPTER 1: INTRODUCTION

Solid organ transplantation is the treatment of choice for end-stage organ failure. Continued function of these grafts is in part dependent upon effective modulation of the recipient's immune system resulting in the suppression of anti-donor responses. Successful immunomodulation is the result of the continuing advances in immunosuppressive therapy. Immunosuppressive drugs used in clinical transplantation fall roughly into three categories and are anti-inflammatory, cytotoxic or inhibit intracellular signaling pathways. Although these drugs effectively prolong graft survival, they are also associated with several undesirable secondary complications including increased risk of opportunistic infections and cancer, renal toxicity, damage to intestinal epithelium, teratogenicity and anemia. Consequently, induction of tolerance to the graft without general immunosuppression remains the ultimate goal in transplantation.

Several experimental protocols that selectively target T cell activation and/or survival have been designed by exploiting the concepts of antigen presentation and costimulation. Historic experiments have shown that pre-transplant donor-specific splenocyte transfusion (DST) improves allograft survival in humans (Brennan et al., 1995). Combination of DST with CD40-CD40L costimulatory blockade utilizing anti-CD40 ligand antibody (anti-CD40L mAb) further prolongs graft survival in mice (Larsen et al., 1996). However, the exact mechanism for tolerance induction by this treatment remains incompletely understood.

1.1 Immunology of Graft Rejection

The immune system is designed to distinguish between "self" and "non-self". During development in the thymus (T cells) or bone marrow (B cells), lymphocytes are exposed to self antigens and are edited or deleted if they either recognize self antigens (B cells) or bind too strongly to self major histocompatibility complex (MHC) molecules (T cells).

Graft rejection is primarily a T cell mediated response. T cells can readily recognize non-self MHC molecules and generate an alloreactive anti-donor response if the donor and recipient MHC differ. The frequency of T cells reactive to non-self MHC molecules is relatively high (1-10%) (Janeway's immunobiology 7th ed), and these differences at MHC loci are a potent trigger of rejection (Valente et al., 1998; Janeway's immunobiology 7th ed.).

Activation of naïve T cells requires both antigen presentation via MHC and costimulatory signals. Antigens are presented by MHC class I and class II molecules expressed on cell surfaces. MHC class I molecules are expressed by most nucleated cells and present intracellular antigens to CD8+ T cells. MHC class II molecules, expressed by professional antigen presenting cells (APCs), present extracellular antigens exclusively to CD4+ T cells. Professional APCs express costimulatory molecules in addition to MHC class II molecules, whereas other cell types express only MHC class I under normal conditions. Under certain

conditions, such as inflammation, MHC class II is expressed on cells of various tissues such as endothelial cells, proximal tubule cells and kidney mesangial cells (Brennan et al., 1995) allowing these cell types to function as "nonprofessional" APCs. This expression of MHC class II molecules in the presence of appropriate costimulatory signals may aid in initiating and/or propagating rejection. On the contrary, in absence of costimulatory signals APCs could cause T cell anergy that may help protect the graft from immune damage (Brennan et al., 1995).

Alloantigen presentation occurs via two pathways. The direct presentation pathway involves donor APCs that travel with the transplanted graft, known as passenger leukocytes, which migrate out of the graft following transplantation and travel to recipient lymph nodes and activate recipient T cells. Direct presentation results in acute rejection and can be avoided by treatment of the graft with antibodies against passenger leukocytes. Indirect alloantigen presentation occurs by recipient APCs taking up and processing allogeneic graft proteins and presenting them to T cells. Relative contributions of these pathways to graft rejection still need to be understood. In context of tolerance induction with DST, a study by Niimi et al. (2000) using haplotype-shared blood as DST suggests that indirect presentation of antigens (presentation of alloantigens in context of self MHC) is essential to induce DST mediated tolerance.

Once activated, graft reactive T cells undergo clonal expansion and mediate a variety of anti-graft responses. For example, activated T cells can activate macrophages, resulting in intra-graft tissue injury and fibrosis. Activated T cells

also move towards B cell follicles, aiding in germinal center formation and providing stimulus for B cells to generate alloantibodies. At a later stage of proliferation, activated T cells differentiate into effector T cells and activate cytotoxic CD8+T cells that further damage the graft tissue.

1.2 Costimulation

Costimulatory signals provided by APCs are necessary to drive the proliferation and differentiation of naïve, graft reactive T cells. Lack of costimulatory signals during antigen presentation induces T cell anergy and/or activation induced cell death (Tan et al., 1993), which could aid in graft survival. Several therapies have been developed on the basis of this concept and target different costimulatory pathways to generate or suppress immune reactions. Some commonly used therapies use CTLA-4 immunoglobulin to inhibit the CD28/B7 costimulatory pathway (Linsley et al., 2009), and antibodies to neutralize the costimulatory molecules OX40L (Croft et al., 2010) and CD70 (McDonagh et al., 2008).

One critical costimulatory pathway required for generating CD4+ T cell responses is the CD40-CD40 ligand (CD40L) interaction (Grewal et al., 1995). Indeed, interruption of this pathway results in long-term allograft survival (senior author Noelle, circa 1994). The CD40-CD40L costimulatory pathway belongs to the Tumor Necrosis Factor (TNF) superfamily and regulates humoral and cellular responses. CD40L (CD154) is expressed on activated T cells and binds to CD40 expressed on APCs. Association of CD40 and CD40L is followed by bidirectional signaling; CD40L sends activating signals to T cells and CD40 induces the APC

to express B7 molecules which further induces activation and proliferation of T cells (Miga et al., 2001; Janeway's immunobiology 7th ed). Hence, this pathway is important not only for generation of T cell responses, but also for B cell activation, Ig isotype switching and germinal centre formation. In context of therapeutic targeting, as CD40L is transiently expressed on activated CD4+ T cells and is rarely expressed on other lymphoid tissues, it is possible to selectively target antigen activated CD4+ T cells by blocking CD40L with anti-CD40L monoclonal antibodies.

1.3 Donor Specific Transfusion

Experiments performed as early as 1972 demonstrate that pre-treatment of allograft recipients with donor-specific blood results in prolonged graft survival in mice (Wood et al., 1984) and humans (Brennan et al., 1995). Some potential mechanisms by which this phenomenon occurs include the induction of T cell anergy as a result of costimulatory signal absence on APC (Schwartz et al., 1990) and the generation of idiotypic antibodies against T cell receptor or MHC (Singhal et al., 1982; Mohanakumar et al., 1987).

However, pretreatment with DST in absence of supportive immunosuppressants also results in the development of cytotoxic T cell reactions and antibodies to donor HLA antigens. The principal concern of DST pretreatment, therefore, was the risk of sensitization instead of tolerance induction (Brennan et al., 1995).

It was later shown that co-administration of DST and anti-CD40L synergistically enhanced allograft survival (Parker et al., 1995; Larsen et al., 1996) and generated experimental transplant tolerance. Since CD40L plays a crucial role in activating humoral responses, costimulatory blockade by anti-CD40L mAb therapy was described as blocking CD4+ T cell help for B cell activation (Noelle RJ et al. 1992) and was also shown to induce tolerance and prolong graft survival (Wood et al.,2008; Bishop et al., 2001). Experiments by Quezada et al. (2003) demonstrated that treatment with DST or anti-CD40L alone modestly prolonged graft survival but in combination prolonged graft survival significantly (Fig. 1). The mechanism for tolerance generated by this treatment remains to be completely defined, and studies regarding this mechanism have used different allograft and transgenic models. Such models suggest anti-CD40L mAb may function by forming a physical barrier to prevent T cells from receiving activation signals (Blazar et al., 1997). Others have found anti-CD40L mAb to drive graft reactive cells to an anergic state without their deletion (Wood et al., 2008, Nathan et al., 2002). Another model used transgenic CD4+ graft reactive T cells (TEa cells) that express a T cell receptor (TCR) specific for donor I-E^d (MHC class II molecule allotype) presented by recipient I-A^b. TEa cells were used to demonstrate that anti-CD40L mAb may mark graft reactive cells for deletion by complement fixation (Sanchez-fueyo et al., 2002). Further, anti-CD40L mAb treatment blocked TEa Tg T cell expansion by approximately 50% (Quezada et al., 2003). Anti-CD40L blockade also exerts profound effects on the longevity, function and differentiation of DCs (Miga et al., 2001). Following DST and anti-

CD40L mAb treatment, graft reactive cells undergo a phase of acute activation and proliferation followed by apoptosis or conversion to regulatory T cells (T_{reg}) in LNs (Burrell et al., 2011). While these experiments give useful insights into the mechanism for tolerance, a clear understanding of this system remains elusive.

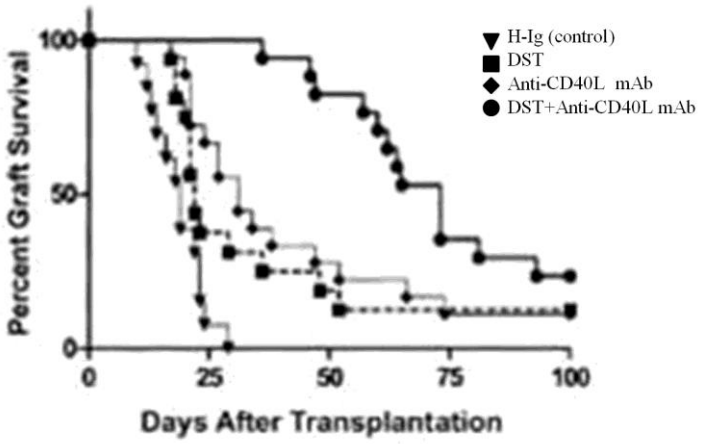

Figure 1: Skin graft rejection by alloreactive TEa Tg T cells delayed by DST+Anti-CD40L mAb treatment. C57BL/6 RAG KO mice were skin grafted (d0) and with injected with DST (d-1). Combined treatment with DST+Anti-CD40L mAb significantly prolonged graft survival as compared to DST or anti-CD40L mAb alone.(Quezada et al., 2003)

1.4 LN Structure

Lymph nodes (LN) are highly organized secondary lymphoid organs (SLO) distributed throughout the body and are linked together by lymphatic vessels. Structurally, LNs are divided into 3 separate regions: the cortex that forms the outer most layer, the paracortex underlying the cortex, and the medulla forming the inner most layer. Macrophages, B cells and follicular dendritic cells (FDC) are arranged in primary follicles in the cortex, and T cells and dendritic cells localize

in the paracortex. Lymphocytes enter paracortical areas from peripheral blood through tiny post-capillary venules (high endothelial venules, HEV) and less often through lymphatic vessels.

The LN is composed of stromal cell subsets that form structural scaffolding, provide architectural support, and contribute to the cellular interactions occurring in the LN (Mueller et al., 2009; Burrell et al. 2011). These stromal cell populations include follicular dendritic cells (FDCs), fibroblastic reticular cells (FRCs), lymphatic endothelial cells (LECs) and blood endothelial cells (BECs).

FRCs form a characteristic dense network around HEVs and guide lymphocyte migration (Katakai et al., 2004(b)). These cells also produce the chemokines CCL19 and CCL21, which have roles in lymphocyte migration (Luther et al., 2000) and CCL2, which prevents lymphocyte homing to LNs (Katakai et al., 2004(a)). FRCs in T cell zones express extracellular components that make up the extra cellular matrix (ECM). These components include ER-TR7 and laminins. ER-TR7 is a fibrous antigen that is detected by the Erasmus University Rotterdan-thymic reticulum antibody 7 (Steele et al., 2009). Laminins are a family of trimeric glycoproteins that are components of the basement membrane and are integral in the formation of the structural scaffolding for most organs. ER-TR7 forms a fibrous meshwork throughout the lymph node. The formation of this intricate meshwork depends on signaling through TNFR and LTβR family cytokines and changes in response to antigen challenge (Katakai et al, 2004).

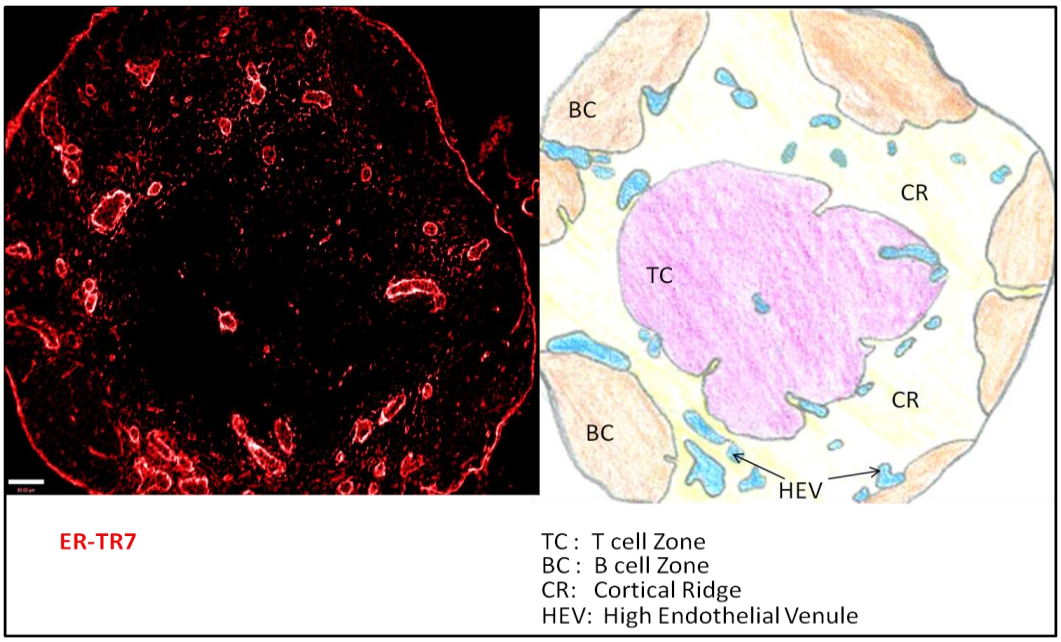

Figure 2: LN structure. Fluorescent IHC (left) and schematic diagram (right) illustrate the basic structural compartments of the LN. Cortical ridge areas between T and B cell zones have FRCs and a dense ERTR7 network. IHC image stained for ER-TR7 in mouse LN; 100x.

HEVs are important for shaping the immune responses as they are sites for lymphocyte entry, and hence molecular interactions between endothelial cells and the entering lymphocytes. Stromal cells lining these HEVs express the chemokines CCL19 and CCL21 (Luther et al., 2000; Forster et al., 2008) that bind to CCR7 on lymphocytes and provide directional cues to these lymphocytes. Moreover, CCL19 and CCL21 expression shapes LN T cell zone (Gunn MD et al., 1999) by attracting DCs and T cells to the T cell zone, where T cells, B cells and DCs interact and shape the adaptive immune response. (Scandella E et al., 2008, Forster et al., 2008).

By producing chemokines, adhesion and structural proteins FRCs not only form physical scaffolding and conduits that allow cells and antigens (Link et al., 2011)

into the LN but also provide cues that dictate the migration and interactions of immune cells that reside in the SLO. These observations suggest a model wherein the lymphoid organ undergoes structural remodeling as the transplant recipient responds to donor antigens (Burrell et al., 2011). Lymphocyte fate depends on the presence on antigen, costimulatory signals, cellular interactions and molecules (chemokines, adhesion molecules) encountered upon entrance in the SLO. LN structure aids in shaping these interactions and, therefore, shapes the subsequent immune response.

Multiple studies for over a decade that have focused on dissecting the signals that determine cell migration and fate indicate that the final outcome of an immune response is influenced heavily by the path leukocytes travel during the immune response (Burrell et al., 2011). Thus, an integrated understanding of spatial and temporal changes occurring during an alloreactive response would provide a better understanding of the complex molecular and cellular events required for graft tolerance, leading to identification of novel therapeutic targets.

CHAPTER 2: MATERIALS AND METHODS

Mice:

All animal procedures were approved by the Institutional Animal Care and Use Committee (IACUC) at the University of Maryland, Baltimore. C57BL/6 (H-2^b) and BALB/c (H-2^d) mice were purchased from the Jackson Laboratory. T cell receptor (TCR)-transgenic (Tg) TEa mice on the C57BL/6 background were obtained from A. Y. Rudensky (Memorial Sloan Kettering Cancer Center, New York, NY, USA). All mice used were female, between 6 and 10 weeks of age and were housed under specific pathogen-free conditions in the University of Maryland Animal Facility. All experiments were performed with age- and sex-matched mice.

In Vivo Treatments:

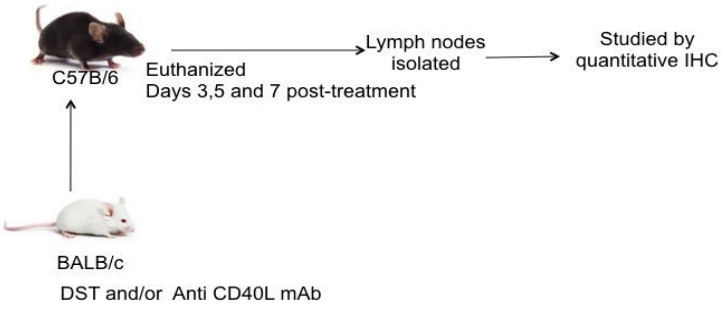

Figure 3: Tolerance induction/ immunization treatments: Tolerance was induced by DST+ anti CD40L m Ab injection (i.v) and immunity was induced by injecting DST only. Mice were euthanized days 3, 5 and 7 post-treatment.

To induce immunity, mice were injected intravenously (i.v.) via tail vein with 10^7 BALB/c splenic lymphocytes (donor specific transfusion, DST). To induce tolerance, mice were injected i.v. via tail vein with DST in conjunction with 0.25mg anti-CD40L mAb (clone MR1, purified by BioXCell, West Lebanon, NH, USA). CD4+ TEa TCR Tg T cells were purified from pooled splenic and LN lymphocytes using the CD4+ negative selection EasySep kit according to the manufacturer's instructions (StemCell Technologies, Vancouver, BC, Canada). Cells were then checked for purity (>90%) and labeled with eFluor 670 (eBioscience, San Diego, CA, USA).

Mouse Dissections:

Mice were euthanized by ketamine-xylazine (200 µl, 100mg/ml ketamine+ 20mg/ml xylazine) injection, i.p (intra peritoneal), followed by cervical dislocation at various time-points (12 hours, 24 hours, 3 days, 5 days and 7 days) post induction of tolerance or immunity, as indicated. Spleens and cervical, brachial, axillary and inguinal lymph nodes (LNs) were isolated.

Immunohistochemistry:

Dissected LNs and spleens were frozen in O.C.T. (optimal cutting temperature) compound (Tissue-Tek). 5µm sections of tissue were cryo-cut and stained with antibodies detecting mouse ER-TR7 (BMA Biomedicals), desmin, laminin (Abcam), collagen III (SouthernBiotech), gp38, CD31 (eBioscience), CCL19, CCL21 (R&D Biosystems) and PNAd (BD Pharmigen) at for 1 hour at room temperature. Secondary antibodies were from Jackson Immunoresearch. Sections were blocked with 5% donkey serum, for donkey-generated secondary antibodies, and/or 5% goat serum for goat-generated secondary antibodies, in PBS (phosphate buffered saline) for 30 minutes. The stained sections were fixed with 3% PFA and quenched with 1% glycerol in PBS. Data are indicative of 3-4 mice/group; 1-3 LN/mouse.

Fluorescence Microscopy:

Fluorescence microscopy of stained sections was done using a Nikon Eclipse E800 biological research microscope equipped with the CFI_{60} optical system, under 4 excitation channels: TRITC, FITC, DAPI and Cy5. 15-20 images were captured per slide (1 slide per mouse for n=1)

Volocity Image Analysis Software:

IHC images were captured and analyzed using Volocity image analysis software from PerkinElmer. Volocity was used to detect positive staining for the indicated marker in the image and analyze its presence in terms of area (μm^2), which can be summarized as the sum (total area staining positive for the indicated marker) or count (number of areas staining positive for the indicated marker) of the analyzed data for the areas detected. For analysis of structural data, the sum of total area staining positive for each structural element for each image was quantified. For chemokine analysis, areas (1 area was approximately equal to 1 cell) staining positive for the chemokine were counted. For TEa cell localization analysis, cortical ridge and T cell areas were marked manually as the region of interest and TEa cells were enumerated.

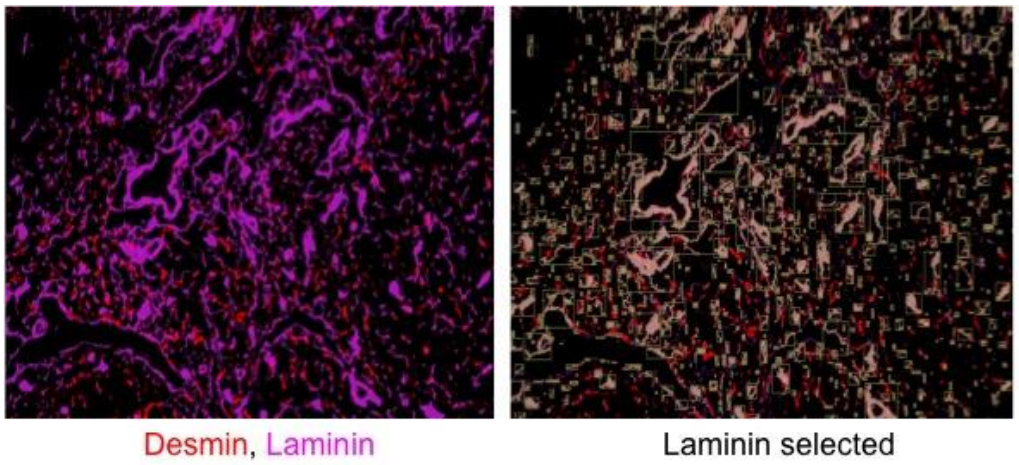

Figure 4: Detection of components using Volocity image analysis software: Total area staining positive in the LN section (total area) was detected based on intensity of the indicated marker in the image analyzed. Representative IHC image stained for desmin and laminin, showing detection of laminin by Volocity image analysis software. 200x.

Cell Preparations:

Isolated spleens were processed into single-cell suspensions using 30μm pore size nylon mesh, treated with ACK lysis buffer (Lonza, Basel, Switzerland) to remove RBCs and cells resuspended in 1× PBS. Isolated LNs were processed using a lymph node stromal cell Librase Blenzyme Digest protocol and CD45- stromal cells were negatively enriched using magnetic separation (MACS, Myltenyi Biotec). Viable cells were enumerated using Trypan blue.

Fluorescence Activated Cell Sorting:

LN stromal cell populations were isolated as described above stained at room temperature with anti-CD45 (clone 30-F11; channel FITC), anti-Podoplanin (gp38, clone eBio8.1.1; channel PE) and anti-CD31 (clone 390; channel APC) from eBioscience. Cells were sorted based on expression of fluorescent markers with a FACSAria at the UMGCC Flow Cytometry Shared services at the University of Maryland, Baltimore. The CD45- cells were sorted as fibroblastic reticular cells (FRCs; gp38+, CD31-), blood endothelial cells (BECs; gp38-, CD31+) and lymphatic endothelial cells (LECs; gp38+, CD31+). Each n-value represents 4 mice for each treatment, with total n-value= 2.

Quantitative Real-Time RT-PCR:

RNA was extracted from sorted stromal cell populations (FRCs, LECs, BECs) using TRIzol reagent. The extracted RNA was treated with DNase I kit (Qiagen), and cDNA was prepared by reverse transcription using the Omniscript Reverse Transcription kit (Qiagen) as indicated in the manufacturer's protocol. Real-time PCR was performed using an ABI Prism 7900 HT Sequence Detection System (Applied Biosciences) with SYBR Green as the reporter (Qiagen). All gene expressions were normalized to the expression of Cyclophylin A.

Statistical Analysis:

GraphPad Prism 4.0c software (California Corporation, CA) was used to analyze immunohistochemistry and quantitative RT-PCR data using one-way ANOVA and Student's unpaired t-tests.

CHAPTER 3: RESULTS

3.1 The LN Structural Components ER-TR7, Desmin, Laminin and Collagen III Change Following Tolerance Induction and Immunization:

Since LN structural components change post antigen challenge (Katakai et al., 2004a) we expected the LN structure to change through the course of response to both tolerance induction and immunization. To assess changes in LN structure during the development of tolerance (treatment with DST and anti-CD40 mAb) vs. immunity (treatment with DST, only), mice were euthanized at days 3, 5 and 7 post-treatment. LNs were isolated and analyzed by quantitative IHC and LN structure was examined via the presence of 4 proteins: ER-TR7, desmin, laminin (secreted by LN stromal cells), and collagen III (col III) that is present in the reticular fibers (Mueller and Gremain, 2009; Burrell et al., 2011). As compared to naïve LNs, the presence of col III, laminin, ER-TR7, and to a lesser extent, desmin increased and showed a distinct peak at day 5 post tolerance induction (Fig. 5b). Laminin and col III expression increased post immunization and peaked at day 5. The amounts of ER-TR7 and desmin remained unchanged over time in immune LNs. Laminin and col III were downregulated at day 3, and levels of all four proteins were close to those observed in naïve LN (baseline) by day 7 following both treatments (Fig. 5b). These data suggest that LN structure undergoes characteristic changes at different time-points following tolerance induction and immunization.

3.2 Distinct Changes in Tolerant And Immune LN Structure:

Since tolerance induction and immunization have different immunological consequences, we expected tolerant and immune LN structures to follow different patterns of structural change when compared to each other. Changes in col III, desmin and laminin remained consistent between tolerant and immune LNs at all time-points. ER-TR7 was significantly upregulated at day 5 following tolerance induction while it remained close to naïve levels following immunization (Fig. 5c). These results demonstrate that the LN structure undergoes distinct changes following the induction of tolerance and immunity, which might aid in defining and shaping the consequent immune response. These data may also indicate that ER-TR7 plays a role in tolerance induction.

a.

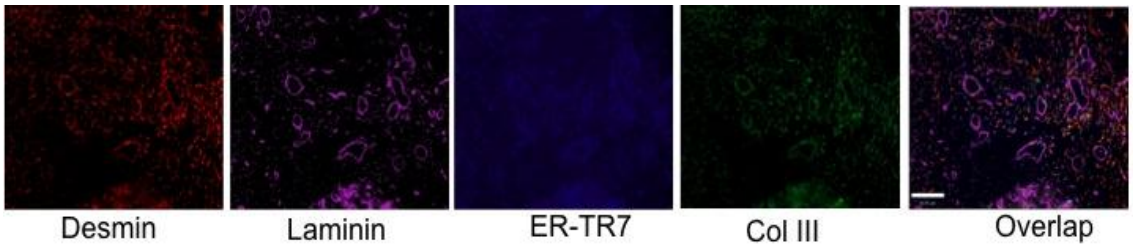
Desmin
Laminin
ER-TR7
Col III
Overlap

b.

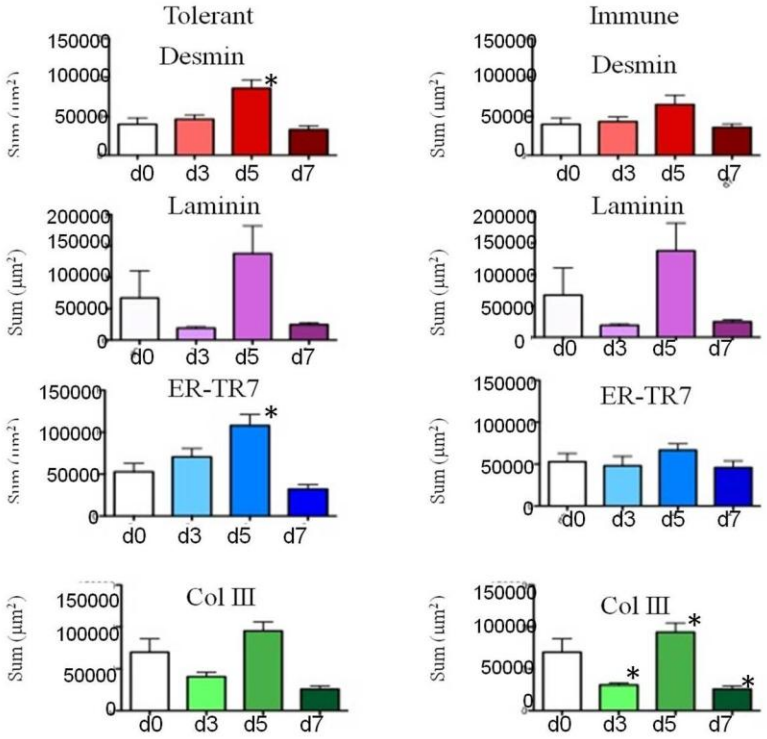
Tolerant
Immune
Desmin
Laminin
ER-TR7
Col III
Sum (µm²)
d0
d3
d5
d7
*

c.

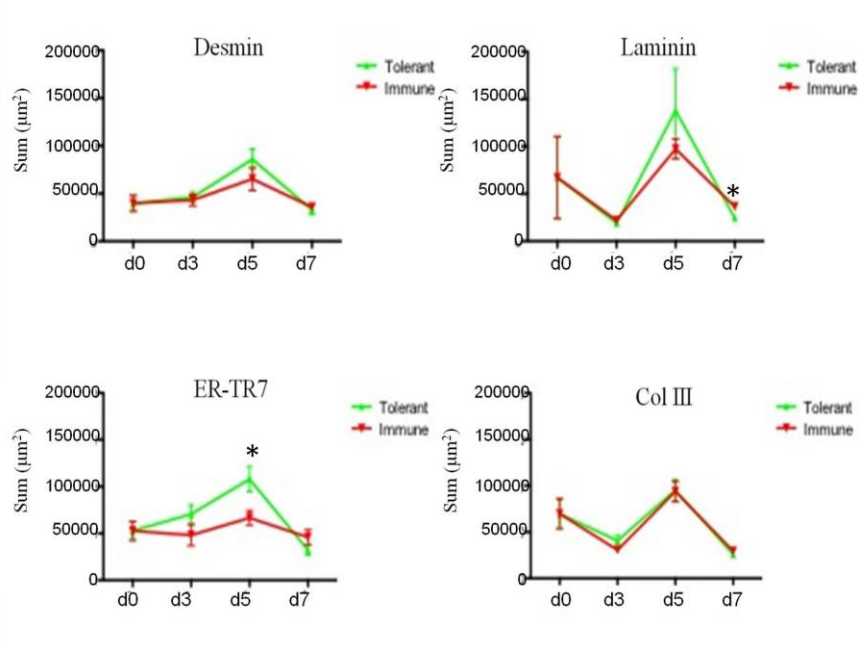

Figure 5: LN structural proteins changed distinctly in tolerant and immune LNs at different time-points: LNs from mice treated with DST (immune) or DST+ anti-CD40L mAb (tolerant) were analyzed for the presence of ER-TR7, desmin, collagen III (col III) and laminin. (a) Representative image to show the structural components in a LN section (image taken from a day 3 immune LN); magnification: 200x (b) LN structural proteins changed at different time-points and peaked at day 5 in tolerant and immune LNs. (c) Tolerant and immune LN structural components in (b) as compared to each other changed differently and exhibited distinct changes, ER-TR7 expression was higher in tolerant LNs at day 5. d0= naïve, (n= 4 mice per group). * represents p values< 0.05 for comparison with naïve LN (b) , for comparison between immune and tolerant LNs at a given time-point. Sum= total area positive for indicated marker (in μm^2).

3.3 CCL19 and CCL21 Chemokine Expression Differs In Tolerant vs. Immune LNs:

Chemokine expression is essential for the recruitment of lymphocytes and affects the consequent immune response. As we focused on the contribution of stromal cells to tolerance induction, we assayed the presence of CCL19 and CCL21, which are expressed by stromal cells and play crucial roles in lymphocyte migration. To assess the chemokine expression profile of the total LN in response to tolerance induction and immunization, isolated LNs were stained for CCL19 and CCL21 and quantified by IHC. At day 3 post-treatment, CCL19 presence increased in immune LNs while it remained close to baseline (naïve level) for tolerant LNs (Fig. 6a). Tolerant and immune LNs showed similar levels of CCL19 at days 5 and 7 post-treatment. Presence of CCL21 was downregulated in tolerant and immune LN when compared to the presence of this chemokine in naïve LN and expressed its lowest level on day 5 (Fig. 6b). These results show delayed upregulation of CCL19 following tolerance induction and indicate that optimal regulation of CCL19 expression might be crucial for inducing tolerance.

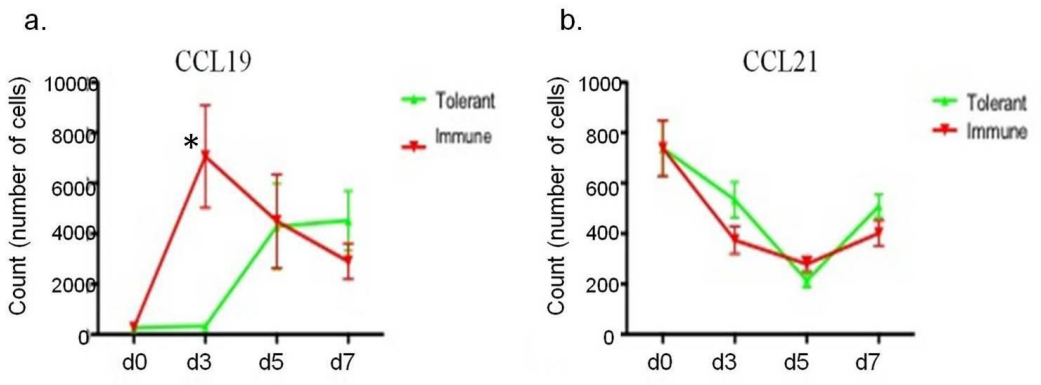

Figure 6: LN expression of CCL19 and CCL21changes following the induction of tolerance and immunity: LNs from tolerant and immune mice were stained and quantified for chemokines CCL19 (a) and CCL21 (b). (a) CCL19 was upregulated at day 3 in immune LNs, and gradually upregulated in tolerant LNs. (b) CCL21 expression decreased for tolerant and immune LNs as compared to naïve. d0 = naïve, (n= 3-4 mice per group). * represents p values< 0.05 (considered significant) for comparison between immune and tolerant LNs at a given time-point. Count = number of cells.

3.4 CCL19 and CCL21 Presence In LN FRCs Differs Under Tolerance And Immunity:

FRCs overlay the LN structural scaffolding and express and produce the chemokines CCL19 and CCL21 (Luther et al., 2000). To assess chemokine presence associated with FRCs, LN sections were stained with CCL19/CCL21, gp38 and CD31, and analyzed by quantitative IHC. Cells staining positive for gp38 and negative for CD31 (gp38+CD31-) were categorized as FRCs. There was no significant change in the proportion of CCL19 expressed by FRCs in immune and tolerant LNs at different time-points; days 3, 5 and 7 (Fig. 7b). The percentage of FRCs positive for CCL21 decreased for immune and tolerant groups, declining the most at day 5 as with total CCL21 presence. At day 7 post-treatment, the percentage of CCL21+FRCs remained lower than naïve levels (baseline) for tolerant LNs and returned to baseline for immune LNs (Fig. 7c). These results show that CCL21 expression is downregulated in tolerant FRCs, which could lead to tolerance induction by limiting lymphocyte migration and interaction.

a.

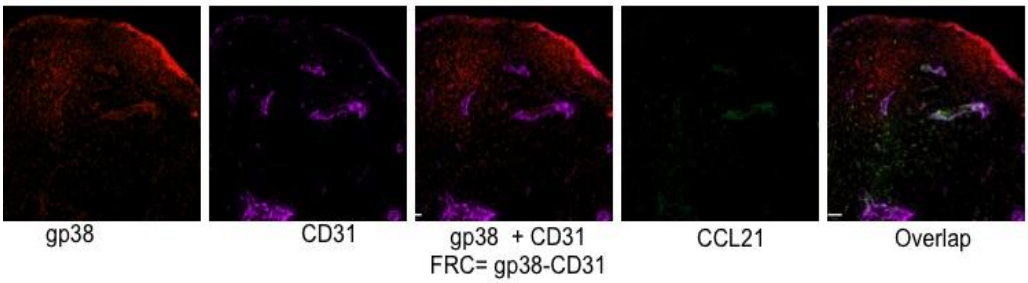

b. c.

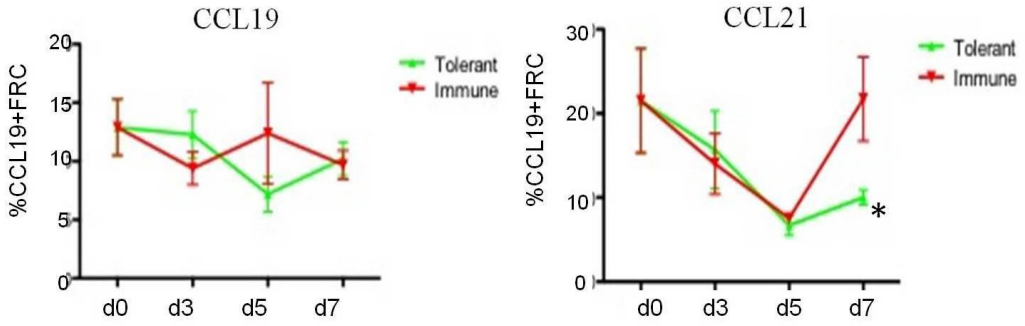

Figure 7: Percentage of FRCs positive for CCL19 and CCL21 in tolerant and immune LNs: LNs from tolerant and immune mice were stained and quantified for chemokines CCL19 and CCL21 with respect to their expression by FRCs. (a) Detection of FRC (gp38+, CD31-) and chemokine+ FRCs in a LN section (image from naïve LN); magnification: 200x (b) The percentage of FRCs that were CCL19+ (%CCL19+FRC) remained similar at all time-points for tolerant and immune LNs. (c) The percentage of FRCs that were CCL21+ (%CCL21+FRC) decreased at day 5 for both groups and remained low for tolerant LNs. d0= naïve, (n= 3-4 mice per group). * represents p values< 0.05 (considered significant) for comparison between immune and tolerant LNs at a given time-point; % of FRC+chemokine= number of FRC+chemokine/ total number of FRCs.

3.5 CCL19 and CCL21 Expression in Tolerant And Immune LN FRCs Differs At 12 Hours Post Antigen Exposure:

CCL19 and CCL21 expressed by stromal cells may affect lymphocyte entry into the LN. At early time-points, expression profiles of CCL19 and CCL21 are important factors for determining the speed and magnitude of lymphocyte entry into the LNs (Forster et al., 2008). To assess these profiles, mice were euthanized 12 hours post tolerance induction or immunization and fluorescently sorted FRCs were analyzed by quantitative RT-PCR. FRCs from tolerant LNs showed lower expression of CCL19 and higher expression of CCL21 as compared to FRCs from immune LNs (Fig. 8a, b). Activation by CCL19 leads to a robust receptor (CCR7) desensitization, unlike activation by CCL21 (Kohout et al., 2004), which might indicate that CCL19 induced signaling is short-lived as compared to CCL21 induced signaling. These data might suggest that tolerant FRCs engage lymphocytes for a longer period of time, although only at earlier time-points, as CCL21 expression seems to be similar for tolerant and immune FRCs at day 3 post-treatment (Fig. 8b).

a. b.

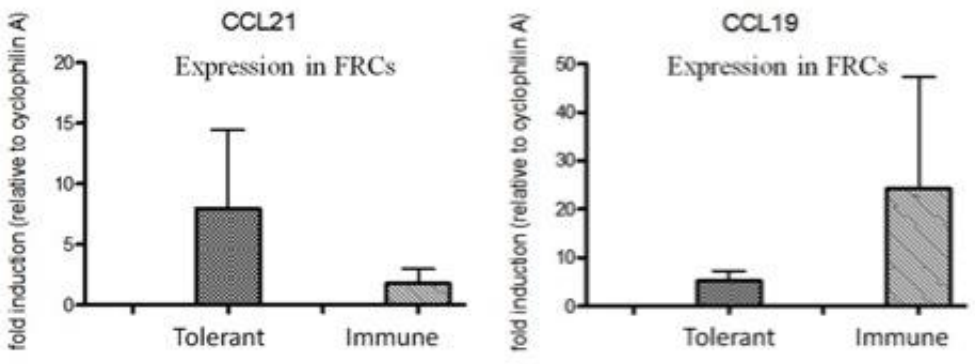

Figure 8: Tolerant and immune LN FRCs upregulate CCL19 12 hours following antigen exposure: LN were sorted for stromal cell populations 12 hours post tolerance induction or immunization, and mRNA for CCL19 (a) and CCL21 (b) were quantified with qRT-PCR. CCL21 expression was upregulated in tolerant FRCs as compared to immune (a), and CCL19 expression was upregulated in immune FRCs as compared to tolerant (b). (n= 2 per group, 4 mice per n value). p values< 0.05 (considered significant) for comparisons between tolerant and immune LNs.

3.6 Graft Reactive Cells Predominantly Localize in CR and T Cell Areas in Tolerant And Immune LNs:

Changes in LN structure and chemokine expression may ultimately affect the fate of graft reactive cells (TEa cells). T cells interact with APCs primarily in the cortical ridge (CR) areas before migrating to T cell areas (Katakai et al., 2004a). Hence, we looked at antigen-specific cell localization in CR and T cell areas. To assess antigen-specific cell localization, TEa cells were labeled with eFluor and injected along with tolerance induction and immunization treatments. Mice were euthanized at 12 hours, 1 day and 3 days post-treatment and LNs were analyzed by quantitative IHC. At 12 hours post-treatment, CR and T cell areas of immune

LNs had more TEa cells as compared to tolerant LNs. TEa cells gradually accumulated in CR and T cell areas of tolerant LNs and were similar to cell numbers observed in immune LNs by day 3 (Fig. 9b). The percentage of TEa cells in the CR and T cell area did not change significantly in both cases. These results show that TEa cells predominantly localize in CR and T cell area (until day 3) under both tolerant and immune conditions. TEa cell entry and migration in tolerant LNs is gradual which might be useful for graft survival. Furthermore, earlier abundance of TEa cells in immune LNs could be a result of elevated CCL19 expression and might lead to earlier TEa cell activation and graft rejection.

a.

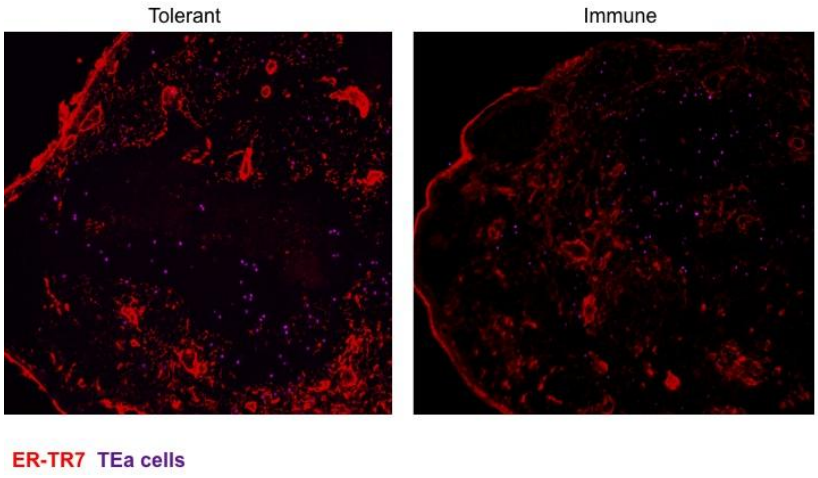

b. c.

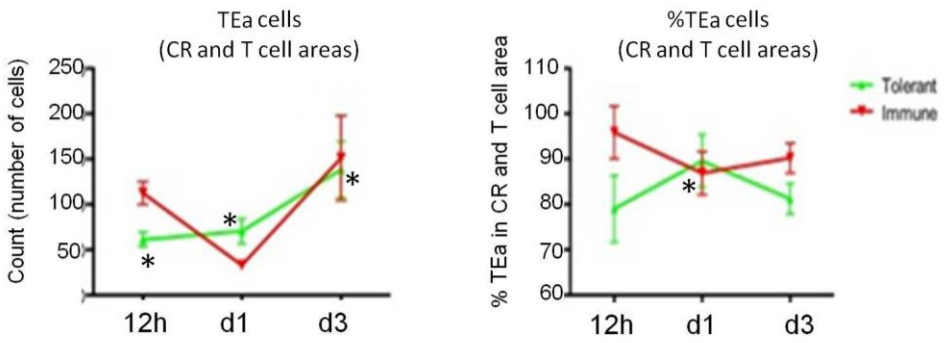

Figure 9: Graft reactive cells predominantly localize in CR and T cell area following tolerance induction and immunization: TEa TCR transgenic CD4+ T cells (TEa cells) were labeled with eFluor and injected with during tolerance induction and immunization. Isolated LNs were analyzed by quantitative IHC for the number of TEa cells present in CR and T cell area. (a) Representative image of graft reactive cell localization in tolerant (left) and immune (right) LNs (12hr time-point); magnification: 100x (b) TEa cells accumulated gradually in CR and T cell area of tolerant LN. (c) Percentage of TEa cells in CR and T cell area = Count of TEa in CR and T cell area/ Total TEa cell count in LN, remained comparable for tolerant and immune LN. (n=2-3 mice per group). * represents p values< 0.05 (considered significant) for comparison between immune and tolernt LNs at a given time-point.

CHAPTER 4: DISCUSSION

In this study, we compared changes in LN structure and chemokine expression as they relate to tolerance and immunity. We assayed two aspects of an immune response: temporal changes in LN structure and chemokine expression, and the effects these changes have on antigen-specific cell location. Our data demonstrated that LN structural components and chemokine expression change over time and are specific to tolerance vs. immunity.

These results expand upon previous experiments describing LN scaffolding as a malleable structure and suggest that it adapts to immune challenge and affects the immune response. FRCs overlay the LN scaffolding and secrete both fibrous proteins and chemokines, consequently affecting cellular interactions within the LN (Mueller and Germain, 2009). They predominantly localize in the paracortex and form structural conduits that allow cells and antigens to flow and migrate within the LN (Link et al., 2011; Pape et al., 2007). Electron microscopy based studies have revealed that FRCs enclose collagen-containing reticular fibers that are composed of extra-cellular matrix (ECM) and make up a 3-dimentional network of extended fibers and cells bodies. These fibers physically interact with immune cells and guide their movement within LN T cell zones (Gretz et al., 1997; Bajenoff et al., 2006).

Immature DCs collect antigens from tissues, carry them to LNs, process the antigens to become mature DCs and present them to T cells (Romani et al., 2001). Lymphocytes entering the LN travel through the FRC conduits where they encounter these mature and immature DCs (Gretz et al., 1996, 1997). Interestingly, immature DCs show higher affinity for ECM fibers than activated DCs (Sixt et al., 2005) and since immature DCs lack costimulatory signals that are essential for T cell activation, they may play role in inducing tolerance (Itano and Jenkins, 2003).

Collagen fibers form the skeletal core of the LN reticular network and maintain the overall LN structure (Gretz et al., 1997). Our results suggest that overall col III expression remains the same for tolerant and immune LNs but increases 5 days post treatment. This upregulation could be as a response to provide structural support for upregulation of other structural components.

FRCs form a layer over ER-TR7+ scaffolds (Link et al., 2011). Expression and distribution of ER-TR7 changes in response to an antigen challenge (Katakai et al., 2004b). Confirming there results, our data showed upregulation in ER-TR7 expression (day 5 post treatment). Interestingly, ER-TR7 upregulation was distinctly pronounced in tolerant LNs.

Many of the ECM components, such as laminin and fibronectin, constitute the reticular fibers that are ligands for integrin adhesion receptors and influence cell movement in vitro (Ahmed et al., 2005). Laminins have been localized to the basement membrane layer of FRCs (Karttunen et al., 1989) and serve as the major

adhesive proteins. They control cellular activities such as migration, proliferation and proliferation by interacting with integrins and other cell surface components (Aumailley et al., 1998). Our results suggest that laminin expression remains the same for tolerant and immune LNs but increases at day 5 post treatment.

Another marker for stromal cells, desmin, is also expressed on FRCs (Mueller and Gremain, 2009). Our data show that desmin expression does not change between tolerant and immune LNs at all time-points. These results collectively suggest that structural components are selectively regulated by FRCs at different time-points under tolerance and immunity.

Moreover, all these structural components are densely packed around the cortical ridge between T cell and B cell areas (Katakai et al., 2004a). DCs entering regional LNs are thought to settle at the CR. In vitro adhesion experiments of DCs to total LNs show higher affinity of DCs for CR as compared to other regions of the LN, which suggests that specific interactions might exist between FRCs and DCs in the CR. (Katakai et al., 2004a). Furthermore, imaging studies indicate the CR region to act as a crossroad for DCs, B cells and T cells. Our structural data, therefore, suggest that the CR areas might be more densely packed under tolerance and might play a role in tolerance induction by diverting the flow of antigen, APCs and naïve and/or activated T cells.

Furthermore, stromal cells also shape immune responses by secreting chemokines, such as CCL19 and CCL21, that affect the migration of APCs and T cells and increasing interactions between them (Luther et al., 2000; Link et al.,

2007; Friedman et al., 2006). CCR7 (the receptor for CCL19 and CCL21) expressed by lymphocytes and mature DCs (Sallusto et al., 1998) mediates signals that are crucial for lymphocyte and DC migration in LNs. CCR7 deficient mice are largely devoid of T cells in their SLOs and show delayed and weakened immune response to an administered antigen (Forster et al., 1999). Interestingly, CCL19 binding to CCR7 causes receptor desensitization, unlike in case of CCL21 (Kohout et al., 2004). These experiments indicate the importance of CCR7 mediated pathways and imply that CCL19 mediated responses may be short lived as compared to those generated to CCL21. Our data showed an initial upregulation of CCL21 (12 hours post treatment) and a delayed upregulation (after day 3) of CCL19 under tolerance as compared to immune LNs where CCL19 was upregulated in FRCs as early as 12 hours post immunization. These results suggest that differential chemokine expression could result in a difference in the speed and intensity of recruitment and homing of naïve T cells and APCs into the LN under tolerance and immunity

Ultimately, the fate of antigen-reactive T cells depends on their interaction with other immune cells and the physical location of these interactions. It has been demonstrated that graft reactive cells have distinct fates depending on the timing, duration and environment of their antigen exposure (Burrell et al., 2011). This current study using graft reactive cells demonstrated that fewer TEa cells traffic into CR of tolerant LNs (as compared to CR of immune LNs) at initial time-points. This observation likely relates to the delayed CCL19 expression under tolerance.

In conclusion, LNs undergo changes with respect to their micro-structure and chemokine expression during an immune response. These functional and temporal changes subsequently choreograph T cell migration and homing to the LN and their interactions with other cell types. Tolerance induction and immunization, therefore, result in unique structural and functional changes indicating LN scaffolding as a malleable structure.

BIBLIOGRAPHY

Ahmed, N., Riley, C., Rice, G., & Quinn, M. (2005). Role of integrin receptors for fibronectin, collagen and laminin in the regulation of ovarian carcinoma functions in response to a matrix microenvironment. *Clinical & Experimental Metastasis, 22*(5), 391-402. doi: 10.1007/s10585-005-1262-y

Aumailley, M., & Smyth, N. (1998). The role of laminins in basement membrane function. *Journal of Anatomy, 193 (Pt 1)*(Pt 1), 1-21.

Bajenoff, M., Egen, J. G., Koo, L. Y., Laugier, J. P., Brau, F., Glaichenhaus, N., & Germain, R. N. (2006). Stromal cell networks regulate lymphocyte entry, migration, and territoriality in lymph nodes. *Immunity, 25*(6), 989-1001. doi: 10.1016/j.immuni.2006.10.011

Bishop, D. K., Chan Wood, S., Eichwald, E. J., & Orosz, C. G. (2001). Immunobiology of allograft rejection in the absence of IFN-gamma: CD8+ effector cells develop independently of CD4+ cells and CD40-CD40 ligand interactions. *Journal of Immunology (Baltimore, Md.: 1950), 166*(5), 3248-3255.

Blazar, B. R., Taylor, P. A., Panoskaltsis-Mortari, A., Buhlman, J., Xu, J., Flavell, R. A., Vallera, D. A. (1997). Blockade of CD40 ligand-CD40 interaction impairs CD4+ T cell-mediated alloreactivity by inhibiting mature

donor T cell expansion and function after bone marrow transplantation. *Journal of Immunology (Baltimore, Md.: 1950), 158*(1), 29-39.

Brennan, D. C., Mohanakumar, T., & Flye, M. W. (1995). Donor-specific transfusion and donor bone marrow infusion in renal transplantation tolerance: A review of efficacy and mechanisms. *American Journal of Kidney Diseases : The Official Journal of the National Kidney Foundation, 26*(5), 701-715.

Burrell, B. E., Ding, Y., Nakayama, Y., Park, K. S., Xu, J., Yin, N., & Bromberg, J. S. (2011). Tolerance and lymphoid organ structure and function. *Frontiers in Immunology, 2*, 64. doi: 10.3389/fimmu.2011.00064; 10.3389/fimmu.2011.00064

Burrell, B. E., Nakayama, Y., Xu, J., Brinkman, C. C., & Bromberg, J. S. (2012). Regulatory T cell induction, migration, and function in transplantation. *Journal of Immunology (Baltimore, Md.: 1950), 189*(10), 4705-4711. doi: 10.4049/jimmunol.1202027; 10.4049/jimmunol.1202027

Croft, M. (2010). Control of immunity by the TNFR-related molecule OX40 (CD134). *Annual Review of Immunology, 28*, 57-78. doi: 10.1146/annurev-immunol-030409-101243; 10.1146/annurev-immunol-030409-101243

Forster, R., Schubel, A., Breitfeld, D., Kremmer, E., Renner-Muller, I., Wolf, E., & Lipp, M. (1999). CCR7 coordinates the primary immune response by

establishing functional microenvironments in secondary lymphoid organs. *Cell, 99*(1), 23-33.

Friedman, R. S., Jacobelli, J., & Krummel, M. F. (2006). Surface-bound chemokines capture and prime T cells for synapse formation. *Nature Immunology, 7*(10), 1101-1108. doi: 10.1038/ni1384

Gretz, J. E., Anderson, A. O., & Shaw, S. (1997). Cords, channels, corridors and conduits: Critical architectural elements facilitating cell interactions in the lymph node cortex. *Immunological Reviews, 156*, 11-24.

Gretz, J. E., Kaldjian, E. P., Anderson, A. O., & Shaw, S. (1996). Sophisticated strategies for information encounter in the lymph node: The reticular network as a conduit of soluble information and a highway for cell traffic. *Journal of Immunology (Baltimore, Md.: 1950), 157*(2), 495-499.

Grewal, I. S., Xu, J., & Flavell, R. A. (1995). Impairment of antigen-specific T-cell priming in mice lacking CD40 ligand. *Nature, 378*(6557), 617-620. doi: 10.1038/378617a0

Gunn, M. D., Kyuwa, S., Tam, C., Kakiuchi, T., Matsuzawa, A., Williams, L. T., & Nakano, H. (1999). Mice lacking expression of secondary lymphoid organ chemokine have defects in lymphocyte homing and dendritic cell localization. *The Journal of Experimental Medicine, 189*(3), 451-460.

Itano, A. A., & Jenkins, M. K. (2003). Antigen presentation to naive CD4 T cells in the lymph node. *Nature Immunology, 4*(8), 733-739. doi: 10.1038/ni957

Junt, T., Scandella, E., & Ludewig, B. (2008). Form follows function: Lymphoid tissue microarchitecture in antimicrobial immune defence. *Nature Reviews.Immunology, 8*(10), 764-775. doi: 10.1038/nri2414; 10.1038/nri2414

Karttunen, T., Sormunen, R., Risteli, L., Risteli, J., & Autio-Harmainen, H. (1989). Immunoelectron microscopic localization of laminin, type IV collagen, and type III pN-collagen in reticular fibers of human lymph nodes. *The Journal of Histochemistry and Cytochemistry : Official Journal of the Histochemistry Society, 37*(3), 279-286.

Katakai, T., Hara, T., Lee, J. H., Gonda, H., Sugai, M., & Shimizu, A. (2004). A novel reticular stromal structure in lymph node cortex: An immuno-platform for interactions among dendritic cells, T cells and B cells. *International Immunology, 16*(8), 1133-1142. doi: 10.1093/intimm/dxh113 (a)

Katakai, T., Hara, T., Sugai, M., Gonda, H., & Shimizu, A. (2004). Lymph node fibroblastic reticular cells construct the stromal reticulum via contact with lymphocytes. *The Journal of Experimental Medicine, 200*(6), 783-795. doi: 10.1084/jem.20040254 (b)

Kohout, T. A., Nicholas, S. L., Perry, S. J., Reinhart, G., Junger, S., & Struthers, R. S. (2004). Differential desensitization, receptor phosphorylation, beta-arrestin recruitment, and ERK1/2 activation by the two endogenous ligands for the CC chemokine receptor 7. *The Journal of Biological Chemistry, 279*(22), 23214-23222. doi: 10.1074/jbc.M402125200

Kramer, R. H., Rosen, S. D., & McDonald, K. A. (1988). Basement-membrane components associated with the extracellular matrix of the lymph node. *Cell and Tissue Research, 252*(2), 367-375.

Larsen, C. P., Elwood, E. T., Alexander, D. Z., Ritchie, S. C., Hendrix, R., Tucker-Burden, C., . . . Pearson, T. C. (1996). Long-term acceptance of skin and cardiac allografts after blocking CD40 and CD28 pathways. *Nature, 381*(6581), 434-438. doi: 10.1038/381434a0

Link, A., Hardie, D. L., Favre, S., Britschgi, M. R., Adams, D. H., Sixt, M., . . . Luther, S. A. (2011). Association of T-zone reticular networks and conduits with ectopic lymphoid tissues in mice and humans. *The American Journal of Pathology, 178*(4), 1662-1675. doi: 10.1016/j.ajpath.2010.12.039; 10.1016/j.ajpath.2010.12.039

Linsley, P. S., & Nadler, S. G. (2009). The clinical utility of inhibiting CD28-mediated costimulation. *Immunological Reviews, 229*(1), 307-321. doi: 10.1111/j.1600-065X.2009.00780.x; 10.1111/j.1600-065X.2009.00780.x

Luther, S. A., Tang, H. L., Hyman, P. L., Farr, A. G., & Cyster, J. G. (2000). Coexpression of the chemokines ELC and SLC by T zone stromal cells and deletion of the ELC gene in the plt/plt mouse. *Proceedings of the National Academy of Sciences of the United States of America, 97*(23), 12694-12699. doi: 10.1073/pnas.97.23.12694

McDonagh, C. F., Kim, K. M., Turcott, E., Brown, L. L., Westendorf, L., Feist, T., Carter, P. J. (2008). Engineered anti-CD70 antibody-drug conjugate with increased therapeutic index. *Molecular Cancer Therapeutics, 7*(9), 2913-2923. doi: 10.1158/1535-7163.MCT-08-0295; 10.1158/1535-7163.MCT-08-0295

Mencacci, A., Perruccio, K., Bacci, A., Cenci, E., Benedetti, R., Martelli, M. F., Romani, L. (2001). Defective antifungal T-helper 1 (TH1) immunity in a murine model of allogeneic T-cell-depleted bone marrow transplantation and its restoration by treatment with TH2 cytokine antagonists. *Blood, 97*(5), 1483-1490.

Miga, A. J., Masters, S. R., Durell, B. G., Gonzalez, M., Jenkins, M. K., Maliszewski, C., Noelle, R. J. (2001). Dendritic cell longevity and T cell persistence is controlled by CD154-CD40 interactions. *European Journal of Immunology, 31*(3), 959-965. doi: 2-A

Mohanakumar, T., Rhodes, C., Mendez-Picon, G., Flye, M. W., & Lee, H. M. (1987). Antiidiotypic antibodies to human major histocompatibility complex

class I and II antibodies in hepatic transplantation and their role in allograft survival. *Transplantation, 44*(1), 54-58.

Mueller, S. N., & Germain, R. N. (2009). Stromal cell contributions to the homeostasis and functionality of the immune system. *Nature Reviews.Immunology, 9*(9), 618-629. doi: 10.1038/nri2588; 10.1038/nri2588

Nathan, M. J., Yin, D., Eichwald, E. J., & Bishop, D. K. (2002). The immunobiology of inductive anti-CD40L therapy in transplantation: Allograft acceptance is not dependent upon the deletion of graft-reactive T cells. *American Journal of Transplantation : Official Journal of the American Society of Transplantation and the American Society of Transplant Surgeons, 2*(4), 323-332.

Niimi, M., Roelen, D. L., Witzke, O., van Rood, J. J., Claas, F. H., & Wood, K. J. (2000). The importance of H2 haplotype sharing in the induction of specific unresponsiveness by pretransplant blood transfusions. *Transplantation, 69*(3), 411-417.

Noelle, R. J., Roy, M., Shepherd, D. M., Stamenkovic, I., Ledbetter, J. A., & Aruffo, A. (1992). A 39-kDa protein on activated helper T cells binds CD40 and transduces the signal for cognate activation of B cells. *Proceedings of the National Academy of Sciences of the United States of America, 89*(14), 6550-6554.

Pape, K. A., Catron, D. M., Itano, A. A., & Jenkins, M. K. (2007). The humoral immune response is initiated in lymph nodes by B cells that acquire soluble antigen directly in the follicles. *Immunity, 26*(4), 491-502. doi: 10.1016/j.immuni.2007.02.011

Parker, D. C., Greiner, D. L., Phillips, N. E., Appel, M. C., Steele, A. W., Durie, F. H., Rossini, A. A. (1995). Survival of mouse pancreatic islet allografts in recipients treated with allogeneic small lymphocytes and antibody to CD40 ligand. *Proceedings of the National Academy of Sciences of the United States of America, 92*(21), 9560-9564.

Quezada, S. A., Fuller, B., Jarvinen, L. Z., Gonzalez, M., Blazar, B. R., Rudensky, A. Y., Noelle, R. J. (2003). Mechanisms of donor-specific transfusion tolerance: Preemptive induction of clonal T-cell exhaustion via indirect presentation. *Blood, 102*(5), 1920-1926. doi: 10.1182/blood-2003-02-0586

Romani, N., Ratzinger, G., Pfaller, K., Salvenmoser, W., Stossel, H., Koch, F., & Stoitzner, P. (2001). Migration of dendritic cells into lymphatics-the langerhans cell example: Routes, regulation, and relevance. *International Review of Cytology, 207*, 237-270.

Sallusto, F., Kremmer, E., Palermo, B., Hoy, A., Ponath, P., Qin, S., Lanzavecchia, A. (1999). Switch in chemokine receptor expression upon TCR

stimulation reveals novel homing potential for recently activated T cells. *European Journal of Immunology, 29*(6), 2037-2045. doi: 2-V

Sanchez-Fueyo, A., Domenig, C., Strom, T. B., & Zheng, X. X. (2002). The complement dependent cytotoxicity (CDC) immune effector mechanism contributes to anti-CD154 induced immunosuppression. *Transplantation, 74*(6), 898-900. doi: 10.1097/01.TP.0000028779.24725.CF

Schwartz, R. H. (1990). A cell culture model for T lymphocyte clonal anergy. *Science (New York, N.Y.), 248*(4961), 1349-1356.

Singal, D. P., & Joseph, S. (1982). Role of blood transfusions on the induction of antibodies against recognition sites on T lymphocytes in renal transplant patients. *Human Immunology, 4*(2), 93-108.

Sixt, M., Kanazawa, N., Selg, M., Samson, T., Roos, G., Reinhardt, D. P., . . . Sorokin, L. (2005). The conduit system transports soluble antigens from the afferent lymph to resident dendritic cells in the T cell area of the lymph node. *Immunity, 22*(1), 19-29. doi: 10.1016/j.immuni.2004.11.013

Steele, K. E., Anderson, A. O., & Mohamadzadeh, M. (2009). Fibroblastic reticular cells and their role in viral hemorrhagic fevers. *Expert Review of Anti-Infective Therapy, 7*(4), 423-435. doi: 10.1586/eri.09.13; 10.1586/eri.09.13

Tan, P., Anasetti, C., Hansen, J. A., Melrose, J., Brunvand, M., Bradshaw, J., Linsley, P. S. (1993). Induction of alloantigen-specific hyporesponsiveness in human T lymphocytes by blocking interaction of CD28 with its natural ligand B7/BB1. *The Journal of Experimental Medicine, 177*(1), 165-173.

Valente, J. F., & Alexander, J. W. (1998). Immunobiology of renal transplantation. *The Surgical Clinics of North America, 78*(1), 1-26.

Wood, M. L., Gottschalk, R., & Monaco, A. P. (1984). Comparison of immune responsiveness in mice after single or multiple donor-specific transfusions. *Journal of Immunology (Baltimore, Md.: 1950), 132*(2), 651-655.

Wood, S. C., Lu, G., Burrell, B. E., & Bishop, D. K. (2008). Transplant acceptance following anti-CD4 versus anti-CD40L therapy: Evidence for differential maintenance of graft-reactive T cells. *American Journal of Transplantation : Official Journal of the American Society of Transplantation and the American Society of Transplant Surgeons, 8*(10), 2037-2048. doi: 10.1111/j.1600-6143.2008.02372.x;